**Nonlinear Functional Analysis and Applications**
**Vol. 29, No. 3 (2024), pp. 711-738**
**ISSN: 1229-1595(print), 2466-0973(online)**

https://doi.org/10.22771/nfaa.2024.29.03.05
http://nfaa.kyungnam.ac.kr/journal-nfaa

# SPATIOTEMPORAL EPIDEMIC MODELS FOR RABIES AMONG DOG WITH VACCINATION APPROACH

**Adil El Alami Laaroussi[1], Amine EL Bhih[2,3] and Mostafa Rachik[2,3]**

[1]Laboratory of Applied Sciences and Didactics, Higher Normal School Tetouan, Abdelmalek Essaadi University, Tetouan, Morocco
e-mail: adilelalamilaaroussi@gmail.com

[2]Laboratory of Analysis Modeling and Simulation, Department of Mathematics and Computer Science, Faculty of Sciences Ben M'Sik, Hassan II University Casablanca, BP 7955, Sidi Othman, Casablanca, Morocco
e-mail: elbhihamine@gmail.com

[3]Multidisciplinary Research and Innovation Laboratory (LPRI), Moroccan School of Engineering Sciences, Casablanca, Morocco

**Abstract.** This study develops an optimal control strategy for canine rabies transmission using a two-dimensional spatiotemporal model with spatial dynamics. Our objective is to minimize the number of infected and exposed individuals while reducing vaccination costs.

We rigorously establish the existence of optimal control and provide a detailed characterization. Numerical simulations show that early intervention, in particular timely vaccination at the onset of an outbreak, effectively controls the disease.

Our model highlights the importance of spatial factors in rabies spread and underlines the need for proactive vaccination campaigns, providing valuable insights for public health policy and intervention strategies.

## 1. Introduction

Rabies is a lethal viral disease that impacts mammals, including humans, by attacking their nervous systems. The virus is responsible for the disease and is commonly transmitted through the saliva of infected animals, either domestic or wild, when they bite or scratch. In addition, contact with saliva

[0]Received October 18, 2023. Revised February 15, 2024. Accepted February 21, 2024.
[0]2020 Mathematics Subject Classification: 47H09, 47H10, 37C25.
[0]Keywords: Spatiotemporal model, rabies between dogs, distributed optimal control, numerical method.
[0]Corresponding author: A. EL Bhih(elbhihamine@gmail.com).

from a rabid animal on the eyes, nose, mouth, or an existing the wound can also cause infection. After contracting the virus, individuals may undergo an the incubation period before showing any symptoms, the duration of the viruss journey to reach the central nervous system can range from several months to several years, depending on the distance, it needs to traverse [14].

The use of infectious disease modeling is a critical mathematical approach to analyzing the epidemiology of infectious diseases to identify and implement effective prevention and control measures. Various models have been utilized to investigate diverse aspects of rabies in both wild animals and humans. Deterministic and continuous models: the work of Anderson and May. In [2], Anderson and May introduced a deterministic SIR model to elucidate the epidemiological characteristics of rabies within fox populations in Europe.

Coyne et al. presented an SEIR-type compartmental model, which has been recently applied by Childs et al [13] to predict the localized dynamics of rabies in raccoons in the United States [13] Dimitrov et al. proposed a model focusing on the immune response to the rabies virus specifically in bats [12] Clayton et al. investigated the optimal control strategies within an SEIRS model that describes the dynamics of epidemic rabies populations in seasonal raccoons. In addition to these deterministic models, discrete deterministic models have also been utilized to study rabies transmission dynamics, as seen in the works of Allen et al. [1], and Artois et al. [3] Furthermore, stochastic models have been employed to explore the complex spatial dynamics of rabies transmission, as demonstrated by Russell et al. [29] and Smith et al. [32]

Once inside the body, the virus quickly spreads through the neural pathways and attacks the central nervous system. From there, it can spread to other organs and cause significant harm by invading multiple tissues. Vaccination against rabies in dogs can be prevented, and for this purpose, several studies have been used to study the effect of this strategy against rabies in dogs or humans [9, 12, 37]. But in these works, the authors use the vaccine as a function of time only. In our work, to give a more realistic study, we use the vaccine in time and space based on the spatiotemporal model [25, 27, 39]. In addition, we extend this one-dimension space model to a two-dimension space model to describe the mobility of the dogs in a spatial area in a significant way. Thus, our study consists of two contributions, the first being to analyze the impact of dog mobilities in dense areas and the second being to apply an optimal vaccine to combat the spread of rabies in a space zone. Similar models of (2.1) can be found in the references ([6, 20]).

Our goal is to design an optimized vaccination program that minimizes both the number of infected individuals and the associated costs of vaccination within a specified timeframe and geographical area. By analyzing the state system and optimal control, we establish the presence of solutions and utilize optimal control theory to describe optimal control in relation to state and adjoint functions. Through numerical simulations, we demonstrate that implementing vaccination control strategies in the spatial domain can significantly curtail the spread of the epidemic within the region for a duration of up to 150 months. The novelty of this article compared to our articles published in scientific journals [21, 22] are: First, the total population in our reaction-diffusion model is unbounded therefore we adopted a mathematical method based on the technique (truncation procedure) to prove the existence of the state system. Second, the system adopted in this work is a four-compartment system; on the other hand in the work that we have published, we used three-compartment systems which required considerable effort from us to carry out an adequate numerical simulation. Finally, for a more realistic scenario in numerical simulation, we assume that the initial infection spreads for 50 months without intervention, considering the progression of the infection at 50 months, we will apply the optimal vaccination at 51 months.

The paper is organized as follows: In Section 2, we present the fundamental mathematical model and its associated optimal control problem. We then move on to Section 3, where we demonstrate the existence of a robust global solution for our system. Section 4 outlines the method used to determine an optimal solution, and Section 5 establishes the necessary optimality conditions. To demonstrate the practical application of our work, we provide numerical results related to our control problem in Section 6. Finally, in Section 7, we conclude the paper.

## 2. The basic mathematical model

2.1. **The model with constant vaccine.** The transmission of the Rabies virus is a serious concern for all mammals, with dogs being the primary carriers that cause the majority of human rabies fatalities in China, according to Rupprecht et al. [28]. Similar trends have been observed in other regions, as reported by Zhang et al. [40]. Unfortunately, Rabies is still prevalent in rural areas of China, as highlighted by Chen et al. [8]. In 1999, only 120 counties reported human rabies cases, but by 2008, the number had increased almost seven times, with the situation worsening in southern provinces and spreading to central and northern regions. To better understand the factors that contribute to the spatial spread of Rabies in mainland China, Ruan et al. developed a model that simulates the transmission of the virus among dogs. [27, 39] used a four-compartment SEIRS model: susceptible, exposed, infected,

and recovered. This model did not consider the impact of dog mobility on the two-dimensional spread of rabie. Inspired by the research conducted by Kim et al. [19] on avian-human influenza epidemic models with diffusion, Settapat Chinviriyasit et al. [11] on numerical modeling of an SIR epidemic model with diffusion, and El Mehdi Lotfi et al. [23] on partial differential equations of an epidemic model with spatial diffusion, where they incorporated partial differential equations (PDEs) to model the spatial spread of diseases, we aim to consider the spatial diffusion of susceptible, exposed, infected and recovered individuals to provide a more realistic depiction of animal mobility.

In our study, we define $\Omega$ as a fixed and bounded domain in $\mathbb{R}^2$ with a smooth boundary $\partial\Omega$, and $\eta$ represents the outward unit normal vector on the boundary. We note the densities susceptible, exposed, infected, and recovered at time $t$ and position $r$ by. $S_d\,(t,r)$ , $E_d\,(t,r)$, $I_d\,(t,r)$, $R_d\,(t,r)$ respectively. So. The resulting model is as follows:

$$\begin{cases} \dfrac{\partial S_d}{\partial t} = \Lambda + \lambda R_d + \sigma\,(1-\gamma)\,E_d - \beta_{dd} S_d I_d - (m+k)\,S_d + d_1 \triangle S_d, \\ \dfrac{\partial E_d}{\partial t} = \beta_{dd} S_d I_d - \sigma\,(1-\gamma)\,E_d - \sigma\gamma E_d - (m+k)\,E_d + d_2 \triangle E_d, \\ \qquad\qquad (t,r) \in Q = [0,T] \times \Omega, \\ \dfrac{\partial I_d}{\partial t} = \sigma\gamma E_d - (m+\mu)\,I_d + d_3 \triangle I_d, \\ \dfrac{\partial R_d}{\partial t} = k\,(S_d + E_d) - (m+\lambda)\,R_d + d_4 \triangle R_d. \end{cases} \tag{2.1}$$

Initial conditions and no-flux boundary conditions are given by

$$\frac{\partial S_d}{\partial \eta} = \frac{\partial E_d}{\partial \eta} = \frac{\partial I_d}{\partial \eta} = \frac{\partial R_d}{\partial \eta} = 0\ , \quad (t,r) \in \Sigma_T = [0,T] \times \partial\Omega, \tag{2.2}$$

$$S_d(0,r) = S_d^0 > 0,\ E_d(0,r) = E_d^0 \geq 0,\ I_d(0,r) = I_d^0 \geq 0$$

and

$$R_d(0,r) = R_d^0 \geq 0\ ,\ r \in \bar{\Omega} \tag{2.3}$$

with $N_d = S_d + E_d + I_d + R_d$, for $t > 0$, $r \in \Omega$, and $d_1$; $d_2$; $d_3$; $d_4$ are the nonnegative diffusion rates. Where the parameters are summarized in Table 1 as follows:

| Parameters | Description |
|---|---|
| $\Lambda$ | Dog birth population |
| $\lambda$ | Dog loss rate of immunity |
| $\gamma$ | Risk of clinical outcome of exposed dogs |
| $\sigma$ | The reciprocal of the dog incubation period |
| $m$ | Dog natural mortality rate |
| $k$ | Dog vaccination rate |
| $\mu$ | Dog disease-related death rate |
| $d_1$ | Diffusion rate for the susceptible dogs |
| $d_2$ | Diffusion rate for the exposed dogs |
| $d_3$ | Diffusion rate for the infected dogs |
| $d_4$ | Diffusion rate for the recovered dogs |

TABLE 1. Description of parameters i in model (2.1)

2.2. **The model with optimal vaccine.** The development of an optimal vaccine is a critical tool in effectively combatting the spread of rabies. Extensive literature exists on optimal control problems related to rabies in mammals, with notable studies by Evans et al. [16], Hampson et al. [17], Kallen et al. [18], Smith et al. [31, 30], Swart et al. [34] and Thulke et al. [35]. However, these studies predominantly focus on employing ordinary differential equation (ODE) systems.

In our research contribution, we advance the field by incorporating a spatiotemporal control strategy in the form of a vaccine, building upon the groundbreaking work of Ruan et al. [27, 39] in their two-dimensional model (as previously discussed). The resulting controlled model is presented as follows:

$$\begin{cases} \dfrac{\partial S_d}{\partial t} = \Lambda + \lambda R_d + \sigma\left(1-\gamma\right)E_d - \beta_{dd}S_dI_d - \left(m + av\left(t,r\right)\right)S_d + d_1\triangle S_d, \\ \dfrac{\partial E_d}{\partial t} = \beta_{dd}S_dI_d - \sigma\left(1-\gamma\right)E_d - \sigma\gamma E_d - \left(m + av\left(t,r\right)\right)E_d + d_2\triangle E_d, \\ \qquad (t,r) \in Q, \\ \dfrac{\partial I_d}{\partial t} = \sigma\gamma E_d - \left(m+\mu\right)I_d + d_3\triangle I_d, \\ \dfrac{\partial R_d}{\partial t} = av\left(t,r\right)\left(S_d + E_d\right) - \left(m+\lambda\right)R_d + d_4\triangle R_d. \end{cases} \tag{2.4}$$

Initial conditions and no-flux boundary conditions are given by

$$\frac{\partial S_d}{\partial \eta} = \frac{\partial E_d}{\partial \eta} = \frac{\partial I_d}{\partial \eta} = \frac{\partial R_d}{\partial \eta} = 0, \quad (t,r) \in \Sigma_T \tag{2.5}$$

$$S_d(0,r) = S_d^0,\ E_d(0,r) = E_d^0,\ I_d(0,r) = I_d^0 \text{ and } R_d(0,r) = R_d^0, \quad r \in \bar{\Omega} \tag{2.6}$$

with the rate at which susceptibles and exposed at location $r$ at time $t$ are effectively vaccinated depends on the quantity of vaccine available, $v(t,r)$, and the vaccine uptake parameter, $a > 0$. Eligible controls are contained in the ensemble

$$U_{ad} = \{v \in L^{\propto}(Q) \,/ 0 \leq v \leq v^{max} < 1, a.e.\,(t,r) \in Q\} \tag{2.7}$$

for some positive constant $v^{max}$ and

$$L^{\propto}(Q) = \{w; Q \to \mathbb{R}; \text{measurable}, s.t.\, |w(t,r)| \leq C, \text{for some } C, a.e.\,(t,r) \in Q\}.$$

Here, our main objective is to minimize the total number of exposed dogs, infected dogs, and to reduce the necessary cost of vaccination. To achieve our goal, we work with the following objective function:

$$J(v) = \int_0^T \int_\Omega \rho_1 E_d(t,r) + \rho_2 I_d(t,r)\, drdt + \frac{\eta}{2} \|v\|^2_{L^2(Q)}. \tag{2.8}$$

We introduce constant weights, $\rho_1$ and $\rho_2$, in our model. The cost of vaccination is a non-linear function of $v$, and we opt for a quadratic function to capture the additional costs associated with high vaccination rates. The parameter $\frac{\eta}{2}$, expressed in units of dogs per square kilometer per square vaccination, serves as a balance between the squared cost of the vaccine and the cost related to the infected population. Consequently, our goal is to determine an optimal control that minimizes a combination of the vaccination cost, the exposed population, and the infectious population over the spatial domain $\Omega$ and a given time period of length $T$ months. To achieve this, we aim to find control functions that satisfy the following optimization criteria:

$$J(v^*) = \min\{J(v),\ v \in U_{ad}\}$$

(1) We put $H = \left(L^2(\Omega)\right)^4$ and $L = L^2([0,T], H)$, we denote by $W^{1,2}$ the space of all absolutely continuous functions $w : [0,T] \to H$ having the property that $\dfrac{\partial w}{\partial t} \in L$.

(2) $F = L^2\left([0,T], H^2(\Omega)\right) \cap L^\infty\left([0,T], H^1(\Omega)\right)$.

## 3. Existence of solution

As the model (2.4)-(2.6) describes the population for biological reasons, the population $S_d$, $E_d$, $I_d$ and $R_d$ should remain nonnegative and bounded. We study in this section the existence of a global strong solution, positivity, and

boundedness of solutions of problem for (2.4)-(2.6). Let $w = (w_1, w_2, w_3, w_4) = (S_d, E_d, I_d, R_d)$ the solution of the system (2.4)-(2.6) with

$$w^0 = \left(w_1^0, w_2^0, w_3^0, w_4^0\right) = \left(S_d^0, E_d^0, I_d^0, R_d^0\right).$$

$A$ denotes the linear operator defined as follows:

$$\begin{aligned} &A:\ D(A) \subset H \longrightarrow H, \\ &Aw = (d_1 \Delta w_1, d_2 \Delta w_2, d_3 \Delta w_3, d_4 \Delta w_4) \in D(A), \\ &w = (w_1, w_2, w_3, w_4) \in D(A) \end{aligned} \tag{3.1}$$

with the domain of $A$ is defined by

$$D(A) = \left\{ w \in \left(H^2(\Omega)\right)^4, \frac{\partial w_1}{\partial \eta} = \frac{\partial w_2}{\partial \eta} = \frac{\partial w_3}{\partial \eta} = \frac{\partial w_4}{\partial \eta} = 0, a.e\, r \in \partial\Omega \right\}, \tag{3.2}$$

where $A$ is a linear operator defined on a Banach space $X$, with the domain $D(A)$ and $g : [0,T] \times X \to X$ is a given function. If $X$ is a Hilbert space endowed with the scalar product $(\cdot, \cdot)$, then the linear operator $A$ is called dissipative if $(Aw, w) \leq 0$ for all $w \in D(A)$.

**Theorem 3.1.** *$X$ be a real Banach space, $A : D(A) \subseteq X \to X$ be the infinitesimal generator of a $C_0-$semigroup of linear contractions $S(t)$, $t \geq 0$ on $X$, and $g : [0,T] \times X \to X$ be a function measurable in $t$ and Lipschitz continuous in $r \in X$, uniformly with respect to $t \in [0,T]$.*

(i) *If $w_0 \in X$, then problem (3.3) admits a unique mild solution, i.e. a function $w \in C([0,T]; X)$ which verifies the equality $w(t) = S(t)w_0 + \int_0^t S(t-s)g(s, w(s))ds$ for all $t \in [0,T]$.*

(ii) *If $X$ is a Hilbert space, $A$ is self-adjoint and dissipative on $X$ and $z_0 \in D(A)$, then the mild solution is in fact a strong solution and $w \in W^{1,2}([0,T]; X) \cap L^2(0,T; D(A))$.*

*Proof.* First recall a general existence result which we use in the sequel (Proposition 1.2, p.175, [5]; see also [26, 36]). Consider the initial value problem

$$\begin{cases} \dfrac{\partial w}{\partial t} = Aw(t) + g(t, w(t)), & t \in [0,T], \\ z(0) = z_0. \end{cases} \tag{3.3}$$

□

We rewrite the problem (2.4)-(2.6) as an abstract problem (3.3). To this end, we denote by

$$\begin{cases} h_1(t,r) = \Lambda + \lambda w_4 + \sigma(1-\gamma) w_2 - \beta_{dd} w_1 w_3 - (m+av) w_1, \\ h_2(t,r) = \beta_{dd} w_1 w_3 - \sigma(1-\gamma) w_2 - \sigma\gamma w_2 - (m+av) w_2, \quad t \in [0,T], \\ h_3(t,r) = \sigma\gamma w_2 - (m+\mu) w_3, \\ h_4(t,r) = av(w_1+w_2) - (m+\lambda) w_4. \end{cases} \tag{3.4}$$

The system (3.4) represent the nonlinear term of (2.4) and we consider the function

$$h(t,w) = (h_1(t,w), h_2(t,w), h_3(t,w), h_4(t,w)), \tag{3.5}$$

then we can rewrite the system (2.4)-(2.6) in the space $H(\Omega)$ as follows

$$\begin{cases} \dfrac{\partial w}{\partial t} = Aw + h(t,w), \qquad t \in [0,T], \\ w(0) = w^0. \end{cases} \tag{3.6}$$

**Theorem 3.2.** *Let $\Omega$ be a bounded domain from $\mathbb{R}^2$, with the boundary smooth enough. As $w_i^0 \geq 0$ on $\Omega$ (for $i = 1,2,3,4$), problem (2.4)-(2.6) has a unique strong solution $w \in W^{1,2}$ such that $w_i \in F \cap L^\infty(Q)$ for $i = 1,2,3,4$. Furthermore, $w_1$, $w_2$, $w_3$ and $w_4$ are nonnegative and bounded uniformly in $L^\infty(Q)$ and there exists $C > 0$ (independent of $v$) such that for a $t \in [0,T]$.*

$$\left\| \frac{\partial w_i}{\partial t} \right\|_{L^2(Q)} + \|w_i\|_L + \|w_i\|_{H^1(\Omega)} + \|w_i\|_{L^\infty(Q)} \leq C \ \text{ for } i = 1,2,3,4. \tag{3.7}$$

*Proof.* Notice that the function $h(t,w)$ defined in (3.5) is not Lipschitz continuous with respect to $w$, uniformly for $t \in [0,T]$. Therefore, we cannot apply Theorem 3.1 for our problem directly.

**Step 1.** This step studies the local existence of positive solutions to system (2.4)-(2.6) in view of Theorem 3.1. We use a truncation procedure for $h$. For a fixed positive integer $k > 0$, let us define the function sets $D_1 = \{z/z > k\}$, $D_2 = \{z/|z| < k\}$, $D_3 = \{z/z < -k\}$ and consider the following auxiliary problem:

$$\begin{cases} \dfrac{\partial w^k}{\partial t} = Aw^k + h^k\left(t, w^k(r,t)\right), \ \text{in } Q, \\ w^k(0,r) = w^0, \ \text{in } \Omega, \end{cases}$$

where $h^k\left(t,w^k\right) = \left(h_1^k\left(t,w^k\right), h_2^k\left(t,w^k\right), h_3^k\left(t,w^k\right), h_4^k\left(t,w^k\right)\right)$.

Here, for each index $i$, $h_i^k\left(t,w^k\right)$ are defined as follows:

$$h_i^k\left(t,w^k\right)=h_i\left(t,[w_1]_{Ds_1},[w_2]_{Ds_2},[w_3]_{Ds_3}\right),$$

where $[w_i]_{Ds_i}$ means that $w_i\in Ds_i$, and

$$[w_i]_{Ds_i}=\begin{cases} k & if\ \ s_i=1,\\ w_i & if\ \ s_i=2,\\ -k & if\ \ s_i=3.\end{cases}$$

As the operator $A$ defined in (3.1)-(3.2) is dissipating, self-adjoint and generates a $C_0$-semi-group of contractions on $M$ [36], it is clear that function $h^k\left(t,w^k\right)$ becomes Lipschitz continuous in $w^k$ uniformly with respect to $t\in[0,T]$. Therefore, Theorem 3.1 assures problem (2.4)-(2.6) admits a unique strong solution $w^k\in W^{1,2}$ with

$$w_1^k,\ w_2^k,\ w_3^k,\ w_4^k\in L. \tag{3.8}$$

In order to show that $w_i^k\in L^\infty(Q)$ for $i=1,\ 2,\ 3,\ 4$, we denote $C_k=\max\left\{\left\|h_1^k\right\|_{L^\infty(Q)},\left\|w_1^0\right\|_{L^\infty(\Omega)}\right\}$ and $\{S(t),t\geq 0\}$ is the $C_0$-semigroup generated by the operator $B:\ D(B)\subset L^2(\Omega)\longrightarrow L^2(\Omega)$, where $Bw_1^k=d_1\Delta w_1^k$ and $D(B)=\left\{w_1^k\in H^2(\Omega),\dfrac{\partial w_1^k}{\partial\eta}=0,\ \ a.e\ \ \partial\Omega\right\}$. It is clear that the function $U_1^k(t,r)=w_1^k-C_kt-\left\|w_1^0\right\|_{L^\infty(\Omega)}$ satisfies the system

$$\begin{cases}\dfrac{\partial U_1^k}{\partial t}(t,r)=d_1\triangle U_1^k+h_1^k\left(t,w^k(t)\right)-C_k,\quad t\in[0,T],\\ U_1^k(0,r)=w_1^0-\left\|w_1^0\right\|_{L^\infty(\Omega)}.\end{cases} \tag{3.9}$$

Note that this system has a solution given by

$$U_1^k(t)=S(t)\left(w_1^0-\left\|w_1^0\right\|_{L^\infty(\Omega)}\right)+\int_0^t S(t-s)\left(h_1^k\left(s,w^k(s)\right)-C_k\right)ds.$$

As $w_1^0-\left\|w_1^0\right\|_{L^\infty(\Omega)}\leq 0$ and $h_1^k\left(s,w^k(s)\right)-C_k\leq 0$, we have $U_1^k(t,r)\leq 0$ for all $(t,r)\in Q$.

Similarly the function $U_2^k(t,r)=w_1^k+C_kt+\left\|w_1^0\right\|_{L^\infty(\Omega)}$ satisfies $U_2^k(t,r)\geq 0$ for all $(t,r)\in Q$. Then

$$\left|w_1^k(t,r)\right|\leq C_kt+\left\|w_1^0\right\|_{L^\infty(\Omega)},\ \forall(t,r)\in Q$$

and analogously, we have

$$\left|w_i^k(t,r)\right|\leq C_kt+\left\|w_i^0\right\|_{L^\infty(\Omega)},\ \ \forall(t,r)\in Q\ \ for\ \ i=2,3,4. \tag{3.10}$$

Thus we have proved that

$$w_i^k \in L^\infty(Q), \ \ \forall\,(t,r) \in Q \ \ for \ \ i=1,2,3,4. \tag{3.11}$$

By the first equation of (2.4), we obtain

$$\begin{aligned}&\int_0^t\int_\Omega \left|\frac{\partial w_1^k}{\partial s}\right|^2 dsdx + d_1^2\int_0^t\int_\Omega \left|\triangle w_1^k\right|^2 dsdx - 2d_1\int_0^t\int_\Omega \frac{\partial w_1^k}{\partial s}\triangle w_1^k dsdx\\ &= \int_0^t\int_\Omega \left(\Lambda + \lambda w_4^k + \sigma\,(1-\gamma)\,w_2^k - \beta_{dd} w_1^k w_3^k - (m+av)\,w_1^k\right)^2 dsdx.\end{aligned}$$

Using the regularity of $w_1^k$ and the Green's formula, we can write

$$2\int_\Omega \frac{\partial w_1^k}{\partial s}\triangle w_1^k dr = -\frac{\partial}{\partial s}\left(\int_\Omega \left|\nabla w_1^k\right|^2 dr\right) ds = -\int_\Omega \left|\nabla w_1^k\right|^2 dr + \int_\Omega \left|\nabla w_1^0\right|^2 dr.$$

Then

$$\begin{aligned}&\int_0^t\int_\Omega \left|\frac{\partial w_1^k}{\partial s}\right|^2 dsdx + d_1^2\int_0^t\int_\Omega \left|\triangle w_1^k\right|^2 dsdx + d_1\int_\Omega \left|\nabla w_1^k\right|^2 dr - d_1\int_\Omega \left|\nabla w_1^0\right|^2 dr\\ &= \int_0^t\int_\Omega \left(\Lambda + \lambda w_4^k + \sigma\,(1-\gamma)\,w_2^k - \beta_{dd} w_1^k w_3^k - (m+av)\,w_1^k\right)^2 dsdx.\end{aligned} \tag{3.12}$$

Since $\left\|w_i^k\right\|_{L^\infty(Q)}$ for $i=1,2,3,4$ are bounded independently of $v$ and $w_1^0 \in H^2(\Omega)$, we deduce that

$$w_1^k \in L^\infty\left([0,T], H^1(\Omega)\right). \tag{3.13}$$

We make use of (3.8), (3.9) and (3.13), in order to get

$$w_1^k \in F \cap L^\infty(Q)$$

and conclude that the inequality in (3.7) holds for $i=1$, similarly for $w_2^k$, $w_3^k$ and $w_4^k$.

In order to show the positiveness of $w_i^k$ for $i=1,2,3,4$, we write the system (2.4) in the form

$$\begin{cases} \dfrac{\partial w_1^k}{\partial t} = d_1\triangle w_1^k + F_1^k\left(w_1^k, w_2^k, w_3^k, w_4^k\right), \\ \dfrac{\partial w_2^k}{\partial t} = d_2\triangle w_2^k + F_2^k\left(w_1^k, w_2^k, w_3^k, w_4^k\right), \quad (t,r) \in Q, \\ \dfrac{\partial w_3^k}{\partial t} = d_3\triangle w_3^k + F_3^k\left(w_1^k, w_2^k, w_3^k, w_4^k\right), \\ \dfrac{\partial w_4^k}{\partial t} = d_4\triangle w_4^k + F_4^k\left(w_1^k, w_2^k, w_3^k, w_4^k\right). \end{cases} \tag{3.14}$$

It is obvious to see that the functions $F_1^k\left(w_1^k, w_2^k, w_3^k, w_4^k\right)$, $F_2^k\left(w_1^k, w_2^k, w_3^k, w_4^k\right)$, $F_3^k\left(w_1^k, w_2^k, w_3^k, w_4^k\right)$, and $F_4^k\left(w_1^k, w_2^k, w_3^k, w_4^k\right)$ are continuously differentiable satisfying $F_1\left(0, w_2^k, w_3^k, w_4^k\right) = \Lambda + \lambda w_4^k + \sigma\left(1-\gamma\right) w_2^k \geq 0$, $F_2^k\left(w_1^k, 0, w_3^k, w_4^k\right) = \beta_{dd} w_1^k w_3^k \geq 0$, $F_3\left(w_1^k, w_2^k, 0, w_4^k\right) = \beta_{dd} w_1^k w_3^k \geq 0$ and $F_4\left(w_1^k, w_2^k, w_3^k, 0\right) = av\left(w_1^k + w_2^k\right) \geq 0$ for all $w_1^k, w_2^k, w_3^k, w_4^k \geq 0$. Since initial data of system (3.14) are nonnegative, we deduce the positivity of $w_1^k$, $w_2^k$, $w_3^k$ and $w_4^k$(see [33]).

Now we particularize $k > 0$ large enough such that

$$C_k\theta + \left\|w_i^0\right\|_{L^\infty(\Omega)} \leq k, i = 1, 2, 3, \text{ for some } \theta \in [0, T]. \tag{3.15}$$

For example, we can take $k > 2\max\left\{\left\|w_i^0\right\|_{L^\infty(\Omega)},\ \ i = 1, 2, 3, 4\right\}$. Let $\theta \in (0, T)$ be maximal with property (3.15). By (3.10)-(3.15), it is clear that $\left|w_i^k(t, r)\right| < k$, for $(t, r) \in [0, \theta] \times \Omega$ and $i = 1, 2, 3$. So, $h^k\left(t, w_1^k, w_2^k, w_3^k, w_4^k\right))$ coincides with $h(t, w_1, w_2, w_3, w_4)$ for$(t, r) \in [0, \theta] \times \Omega$, and consequently $w^k = \left(w_1^k, w_2^k, w_3^k, w_4^k\right)$ is a local solution for (2.4)-(2.6) defined on $[0, \theta] \times \Omega$.

**Step 2.** It remains to show that the above local positive solution of problem (2.4)-(2.6) is in fact a global one in $[0, \theta] \times \Omega$. Indeed, it is sufficient to show the uniformly boundedness of $w_i, i = 1, 2, 3, 4$ in $[0, \theta] \times \Omega$. To this end, we first introduce $Z = w_1 + w_2 + w_3 + w_4$, then

$$\frac{\partial Z}{\partial t} = d_1 \triangle w_1 + d_2 \triangle w_2 + d_3 \triangle w_3 + d_4 \triangle w_4 + \Lambda - mZ,$$

we have $\dfrac{\partial Z}{\partial t} - d\triangle Z \leq \Lambda - mZ$ with $d = 4\max\left\{d_1, d_2, d_3, d_4\right\}$ and $0 < Z\left(0, r\right) \leq \left\|Z\left(0, r\right)\right\|_{L^\infty(\Omega)}$. This leads to the estimate $0 < Z\left(t, r\right) \leq \overline{Z}\left(t\right)$, $(t, r) \in [0, \theta] \times \Omega$, where $\overline{Z}\left(t\right) = \left[\frac{\Lambda}{d} + \left(\left\|\overline{Z}\left(0, r\right)\right\|_{L^\infty(\Omega)} - \frac{\Lambda}{d}\right) e^{-td}\right]$ is the solution of the problem

$$\begin{cases} \dfrac{\partial \overline{Z}}{\partial t} = \Lambda - m\overline{Z}, \\ \\ \overline{Z}\left(0\right) = \left\|Z\left(0, r\right)\right\|_{L^\infty(\Omega)}. \end{cases}$$

Hence, we have

$$0 < \overline{Z}\left(t\right) \leq \max\left\{\left\|N\left(0, r\right)\right\|_{L^\infty(\Omega)}, \frac{\Lambda}{d}\right\}$$

for $t \in [0, \theta]$ and thus

$$0 < Z\left(t, r\right) \leq \max\left\{\left\|Z\left(0, r\right)\right\|_{L^\infty(\Omega)}, \frac{\Lambda}{d}\right\}.$$

Therefore, $\|Z\|_{L^\infty([0,\theta]\times\Omega)} \leq m_1$ for some $m_1 > 0$ independent of $k$ and of $v$. Next, we can deduce the boundedness of $w_1$, $w_2$, $w_3$ and $w_4$ on $[0,\theta] \times \Omega$. Consequently, $w_i$ are defined on the whole set $Q$ (and also positive and bounded). Thus $(w_1, w_2, w_3, w_4)$ is a global positive strong solution of system (2.4)-(2.6) and it satisfies (3.7). This completes the proof. □

## 4. The existence of the optimal solution

In this section, we will prove the existence of an optimal control for the problem (2.8) subject to reaction diffusion system (2.4)-(2.6) and $v \in U_{ad}$. The main result of this section is the following:

**Theorem 4.1.** *Let $\Omega$ be a bounded domain from $\mathbb{R}^2$, with the boundary smooth enough. As $w_i^0 \geq 0$ on $\Omega$ (for $i = 1\,, 2,\ 3,\ 4$), $\lambda$, $\mu$, $\sigma$, $\gamma$, $\beta_{dd}$, $m$, $k \geq 0$, $v \in U_{ad}$, and $w \in D(A)$. Then the optimal control problem* (2.4)-(2.8) *admits an optimal solution $(w^*, v^*)$.*

*Proof.* From Theorem 3.2, we know that, for every $v \in U_{ad}$, there exists a unique solution $(w_1, w_2, w_3, w_4)$ to system (2.4)-(2.6). Assume that

$$\inf_{v\in U_{ad}} J(v) > -\infty.$$

Let $\{v^n\} \subset U_{ad}$ be a minimizing sequence such that

$$\lim_{n\to\infty} J(v^n) = \inf_{v\in U_{ad}} J(v),$$

where $(w_1^n, w_2^n, w_3^n, w_4^n)$ is the solution of system (2.4)-(2.6) corresponding to the control $(v^n)$ for $n = 1, 2, \ldots$. That is,

$$\begin{cases} \dfrac{\partial w_1^n}{\partial t} = d_1\Delta w_1^n + \Lambda + \lambda w_4^n + \sigma(1-\gamma) w_2^n - \beta_{dd} w_1^n w_3^n - (m + av^n) w_1^n, \\ \dfrac{\partial w_2^n}{\partial t} = d_2\Delta w_2^n + \beta_{dd} w_1^n w_3^n - \sigma(1-\gamma) w_2^n - \sigma\gamma w_2^n - (m+av^n) w_2^n\ ,\ (t,r) \in Q, \\ \dfrac{\partial w_3^n}{\partial t} = d_3\Delta w_3^n + \sigma\gamma w_2^n - (m+\mu) w_3^n, \\ \dfrac{\partial w_4^n}{\partial t} = d_4\Delta w_4^n + av^n (w_1^n + w^n{}_2) - (m+\lambda) w_4^n. \end{cases} \tag{4.1}$$

$$\frac{\partial w_1^n}{\partial \eta} = \frac{\partial w_2^n}{\partial \eta} = \frac{\partial w_3^n}{\partial \eta} = \frac{\partial w_4^n}{\partial \eta} = 0, \quad (t,r) \in \Sigma\,(t,r) \in \Sigma, \tag{4.2}$$

$$w_i^n(0,r) = w_i^0 \ \textit{for}\ i = 1,2,3,4, \qquad r \in \Omega. \tag{4.3}$$

By Theorem 3.2 using the estimate (3.7) of the solution $w_i^n$, there exists a constant $C > 0$ such that for all $n \geq 1$, $t \in [0,T]$,

$$\left\| \frac{\partial w_i^n}{\partial t} \right\|_{L^2(Q)} \leq C,\ \|w_i^n\|_{L^2([0,T],H^2(\Omega))} \leq C,\ \|w_i^n\|_{H^1(\Omega)} \leq C,\ i = 1,2,3,4. \tag{4.4}$$

$H^1(\Omega)$ is compactly embedded in $L^2(\Omega)$, so we deduce that $w_1^n(t)$ is compact in $L^2(\Omega)$.

Let's show that $\{w_1^n(t), n \geq 1\}$ is equicontinuous in $C\left([0,T], L^2(\Omega)\right)$. As $\dfrac{\partial w_1^n}{\partial t}$ is bounded in $L^2(Q)$, this implies that for all $s,t \in [0,T]$,

$$\left| \int_\Omega (w_1^n)^2(t,r)\,dr - \int_\Omega (w_1^n)^2(s,r)\,dr \right| \leq K|t-s|. \tag{4.5}$$

Then, the Ascoli-Arzela Theorem (see, [7]) implies that $w_1^n$ is compact in $C([0,T], L^2(\Omega))$. Hence, selecting further sequences, if necessary, we have $w_1^n \longrightarrow w_1^*$ in $L^2(\Omega)$, uniformly with respect to $t$ and analogously, we have for $w_i^n \longrightarrow w_i^*$ in $L^2(\Omega)$ for $i = 2,3,4$ uniformly with respect to $t$.

From the boundedness of $\Delta w_i^n$ in $L^2(Q)$, which implies it is weakly convergent in $L^2(Q)$ on a subsequence denoted again $\triangle w_i^n$ then for all distribution $\varphi$

$$\int_Q \varphi \Delta w_i^n = \int_Q w_i^n \triangle\varphi \to \int_Q w_i^* \triangle\varphi = \int_Q \varphi \Delta w_i^*,$$

which implies that $\triangle w_i^n \to \triangle w_i^*$ weakly in $L^2(Q)$, $i = 1, 2, 3, 4$. In addition, the estimates (4.4) leads to

$$\begin{aligned}
&\frac{\partial w_i^n}{\partial t} \to \frac{\partial w_i^*}{\partial t} \text{ weakly in } L^2(Q), i = 1, 2, 3, 4,\\
&w_i^n \to w_i^* \text{ weakly in } L^2\left(0,T; H^2(\Omega)\right), i = 1, 2, 3, 4,\\
&w_i^n \to w_i^* \text{ weakly star in } L^\infty\left(0,T; H^1(\Omega)\right), i = 1, 2, 3, 4.
\end{aligned}$$

We now show that $w_1^n w_3^n \mapsto w_1^* w_3^*$ strongly in $L^2(Q)$, we write

$$w_1^n w_3^n - w_1^* w_3^* = (w_1^n - w_1^*) w_3^n + w_1^* (w_3^n - w_3^*)$$

and we make use of the convergences $w_i^n \longrightarrow w_i^*$ strongly in $L^2(Q)$, $i = 1, 3$ and of the boundedness of $w_1^n$, $w_3^n$ in $L^\infty(Q)$, then $w_1^n w_3^n \mapsto w_1^* w_3^*$ strongly in $L^2(Q)$.

Since $v^n$ is bounded, we can assume that $v^n \to v^*$ weakly in $L^2(Q)$ on a subsequence denoted again $v^n$. Since $U_{ad}$ is a closed and convex set in $L^2(Q)$, it is weakly closed, so $v^* \in U_{ad}$ .

We now show that $v^n w_i^n \to v^* w_i^*$ weakly in $L^2(Q)$ for $i = 1,2$. Writing

$$v^n w_i^n - v^* w_i^* = (w_i^n - w_i^*) v^n + (v^n - v^*) w_i^*,\ i = 1,2$$

and making use of the convergences $w_i^n \longrightarrow w_i^*$ strongly in $L^2(Q)$ for $i = 1, 2$ and $v_i^n \longrightarrow v_i^*$ weakly in $L^2(Q)$, for $i = 1, 2$, one obtains that $v^n w_i^n \to v^* w_i^*$ weakly in $L^2(Q)$ for $i = 1, 2$.

By taking $n \to \infty$ in (4.1)-(4.3), we obtain that $w^*$ is a solution of (2.4)-(2.6) corresponding to $v^* \in U_{ad}$. Therefore,

$$\begin{aligned} J(v^*) &= \int_0^T \int_\Omega \rho_1 w_2^*(t,r)\, drdt + \int_0^T \int_\Omega \rho_2 w_3^*(t,r)\, drdt + \frac{\eta}{2} \|v^*\|^2_{L^2(Q)} \\ &\leq \liminf_{n \to \infty} \left( \int_0^T \int_\Omega \rho_1 w_2^n(t,r)\, drdt + \int_0^T \int_\Omega \rho_2 w_3^n(t,r)\, drdt + \frac{\eta}{2} \|v^n\|^2_{L^2(Q)} \right) \\ &= \lim_{n \to \infty} \left( \int_0^T \int_\Omega \rho_1 w_2^n(t,r)\, drdt + \int_0^T \int_\Omega \rho_2 w_3^n(t,r)\, drdt + \frac{\eta}{2} \|v^n\|^2_{L^2(Q)} \right) \\ &= \inf_{v \in U_{ad}} J(v). \end{aligned}$$

This shows that $J$ attains its minimum at $(w^*, v^*)$, we deduce that $(w^*, v^*)$ verifies problem (2.4)-(2.6) and minimizes the objectif functional (2.8). This completes the proof. □

## 5. Necessary optimality conditions

Let

$$H = \begin{pmatrix} -\beta_{dd} w_3^* - m - a v^* & \sigma(1-\gamma) & -\beta_{dd} w_1^* & \lambda \\ \beta_{dd} w_3^* & -\sigma(1-\gamma) - \sigma\gamma - m - a v^* & \beta_{dd} w_1^* & 0 \\ 0 & \sigma\gamma & -m - \mu & 0 \\ a v^* & a v^* & 0 & -m - \lambda \end{pmatrix}$$

and

$$G = \begin{pmatrix} -a w_1^* \\ -a w_2^* \\ 0 \\ a w_1^* + a w_2^* \end{pmatrix}$$ in this section.

Then we characterize the optimality system.

First, we need the Gateaux differentiability of the mapping $v \to w(v)$, proved by the theorem:

**Theorem 5.1.** *The mapping $w : U_{ad} \to W^{1,2}$ with $w_i \in N(T, \Omega)$ for $i = 1, 2, 3, 4$ is Gateaux differentiable with respect to $v^*$. For all direction $v \in L^2(Q)$, $w'(v^*)\, v = W$ is the unique solution in $W^{1,2}$ with $W_i \in N$ of the*

*following equation*

$$\begin{cases} \dfrac{\partial W}{\partial t} = AW + HW + Gv, \quad t \in [0,T], \\ \\ W(0,r) = 0, \end{cases} \tag{5.1}$$

*where* $W = (W_1, W_2, W_3, W_4)$.

*Proof.* Denote by

$$w^\varepsilon = (w_1^\varepsilon, w_2^\varepsilon, w_3^\varepsilon, w_4^\varepsilon) = (w_1, w_2, w_3, w_4)(v^\varepsilon)$$

and

$$w^* = (w_1^*, w_2^*, w_3^*, w_4^*) = (w_1, w_2, w_3, w_4)(v^*)$$

the solution of (2.4)-(2.6) corresponding to $v^\varepsilon$ and $v^*$ respectively, where $(w^*, v^*)$ is an optimal pair such that $v^\varepsilon = v^* + \varepsilon v \in U_{ad}$ (for $\varepsilon > 0$ small) and $v \in \left(L^2(Q)\right)^2$.

We put $W_i^\varepsilon = \dfrac{w_i^\varepsilon - w_i^*}{\varepsilon}$ for $i = 1, 2, 3, 4$.

We denote $S^\varepsilon$ the system (2.4)-(2.6) corresponding to $v^\varepsilon$, and $S^*$ the system (2.4)-(2.6) corresponding to $v^*$, subtracting system $S^\varepsilon$ from $S^*$, we have

$$\begin{cases} \dfrac{\partial W_1^\varepsilon}{\partial t} = d_1 \Delta W_1^\varepsilon - (\beta_{dd} w_3^\varepsilon + m + a v^\varepsilon) W_1^\varepsilon + \sigma(1-\gamma) W_2^\varepsilon \\ \qquad\qquad -\beta_{dd} w_1^* W_3^\varepsilon + \lambda W_4^\varepsilon - a v^* w_1^*, \\ \\ \dfrac{\partial W_2^\varepsilon}{\partial t} = d_2 \Delta W_2^\varepsilon + \beta_{dd} w_3^\varepsilon W_1^\varepsilon - (\sigma(1-\gamma) + \sigma\gamma + m + a v^\varepsilon) W_2^\varepsilon \\ \qquad\qquad +\beta_{dd} w_1^* W_3^\varepsilon - a v^* w_2^*, \\ \\ \dfrac{\partial W_2^\varepsilon}{\partial t} = d_3 \Delta W_2^\varepsilon + \sigma\gamma W_2^\varepsilon - (m+\mu) W_3^\varepsilon, \qquad\qquad (r,t) \in Q, \\ \\ \dfrac{\partial W_3^\varepsilon}{\partial t} = d_4 \Delta W_3^\varepsilon + a v^\varepsilon (W_1^\varepsilon + W_2^\varepsilon) - (m+\lambda) W_4^\varepsilon + a v^* w_1^* + a v^* w_2^*, \end{cases} \tag{5.2}$$

with the homogeneous Neumann boundary conditions

$$\frac{\partial W_1^\varepsilon}{\partial \eta} = \frac{\partial W_2^\varepsilon}{\partial \eta} = \frac{\partial W_3^\varepsilon}{\partial \eta} = \frac{\partial W_3^\varepsilon}{\partial \eta} = 0, \quad (r,t) \in \Sigma, \tag{5.3}$$

$$W_i^\varepsilon(0,r) = 0, \quad r \in \Omega \ \ for\ i = 1,2,3,4. \tag{5.4}$$

We prove that $W_i^\varepsilon$ are bounded in $L^2(Q)$ uniformly with respect to $\varepsilon$. For this end, we put by

$W^\varepsilon = (W_1^\varepsilon, W_2^\varepsilon, W_3^\varepsilon, W_4^\varepsilon)$,

$$H = \begin{pmatrix} -\beta_{dd} w_3^{\varepsilon} - m - a v^{\varepsilon} & \sigma(1-\gamma) & -\beta_{dd} w_1^{*} & \lambda \\ \beta_{dd} w_3^{\varepsilon} & -\sigma(1-\gamma) - \sigma\gamma - m - a v^{\varepsilon} & \beta_{dd} w_1^{*} & 0 \\ 0 & \sigma\gamma & -m-\mu & 0 \\ a v^{\varepsilon} & a v^{\varepsilon} & 0 & -m-\lambda \end{pmatrix}$$

and

$$G = \begin{pmatrix} -a w_1^{*} \\ -a w_2^{*} \\ 0 \\ a y_1^{*} + a y_2^{*} \end{pmatrix}, \text{ then we can rewrite system (5.2) as}$$

$$\begin{cases} \dfrac{\partial W^{\varepsilon}}{\partial t} = A W^{\varepsilon} + H Y^{\varepsilon} + G v, \quad t \in [0,T], \\ \\ W^{\varepsilon}(0,r) = 0. \end{cases} \tag{5.5}$$

If $(S(t), t \geq 0)$ is the semigroup generated by $A$, then the solution of (5.5) can be expressed as

$$W^{\varepsilon}(t) = \int_0^t S(t-s) H^{\varepsilon}(s) W^{\varepsilon}(s)\, ds + \int_0^t S(t-s) G v(s)\, ds. \tag{5.6}$$

On the other hand the coefficients of the matrix $H^{\varepsilon}$ are bounded uniformly with respect to $\varepsilon$, using Gronwall's inequality, we have

$$\|W_i^{\varepsilon}\|_{L^2(Q)} \leq \beta, \tag{5.7}$$

where $\beta > 0$ $(i = 1,2,3,4)$. Then

$$\|w_i^{\varepsilon} - w_i^{*}\|_{L^2(Q)} = \varepsilon \|W_i^{\varepsilon}\|_{L^2(Q)}. \tag{5.8}$$

Hence $w_i^{\varepsilon} \to w_i^{*}$ in $L^2(Q)$, $i = 1,2,3,4$.

We put

$$H = \begin{pmatrix} -\beta_{dd} w_3^{*} - m - a v^{*} & \sigma(1-\gamma) & -\beta_{dd} w_1^{*} & \lambda \\ \beta_{dd} w_3^{*} & -\sigma(1-\gamma) - \sigma\gamma - m - a v^{*} & \beta_{dd} w_1^{*} & 0 \\ 0 & \sigma\gamma & -m-\mu & 0 \\ a v^{*} & a v^{*} & 0 & -m-\lambda \end{pmatrix}$$

and $W = (W_1, W_2, W_3, W_4)$. Then the system (5.2)-(5.4) can be written in the form

$$\begin{cases} \dfrac{\partial W}{\partial t} = A W + H W + G u, \qquad t \in [0,T], \\ \\ W(0) = 0. \end{cases} \tag{5.9}$$

and its solution can be expressed as

$$W(t) = \int_0^t S(t-s) H(s) W(s)\, ds + \int_0^t S(t-s) Gv(s)\, ds. \tag{5.10}$$

By (5.6) and (5.10) one deduces that

$$W^{\varepsilon}(t) - W(t) = \int_0^t S(t-s) H^{\varepsilon}(s) (W^{\varepsilon} - W)(s) + W(s) (H^{\varepsilon}(s) - H(s))\, ds. \tag{5.11}$$

Thus all the coefficients of the matrix $H^{\varepsilon}$ tend to the corresponding coefficients of the matrix $H$ in $L^2(Q)$. An application of Gronwall's inequality yields to $W_i^{\varepsilon} \to W_i$ in $L^2(Q)$ as $\varepsilon \to 0$ for $i = 1, 2, 3, 4$. □

Let $v^*$ be an optimal control of (2.4)-(2.8), $w^* = (w_1^*, w_2^*, w_3^*, w_4^*)$ be the optimal state, $D$ be the matrix defined by $D = \begin{pmatrix} 0 & 0 & 0 & 0 \\ 0 & 1 & 0 & 0 \\ 0 & 0 & 1 & 0 \\ 0 & 0 & 0 & 0 \end{pmatrix}$, $D^*$ be the adjoint matrix associated to $D$, $H^*$ be the adjoint matrix associated to $H$, $\rho^* = (0, \rho_1, \rho_2, 0)$ and $p = (p_1, p_2, p_3, p_4)$ the adjoint variable, the dual system associated to the system (2.4)-(2.8) given by

$$\begin{cases} -\dfrac{\partial p}{\partial t} - Ap - H^* p = D^* D\rho, \quad t \in [0, T], \\ \\ p(T, r) = 0. \end{cases} \tag{5.12}$$

**Lemma 5.2.** *Given the assumptions of Theorem* 3.2*, if* $(w^*, v^*)$ *is an optimal pair, then there exists a unique strong solution* $p \in W^{1,2}$ *to the system* (5.12) *with* $p_i \in N$ *for* $i = 1, 2, 3, 4$.

*Proof.* Similar to the approach used in Theorem (3.2), we introduce the change of variable $s = T - t$ and define $q_i(s, r) = p_i(T - s, r) = p_i(t, r)$ for $(t, r) \in Q$ and $i = 1, 2, 3, 4$. By applying this transformation, we can establish the existence of a solution to this lemma. □

To derive the necessary conditions for the optimal control problem, we employ standard optimization techniques. By analyzing the objective functional, exploring the relationships between the state and adjoint equations, and utilizing the properties of the system, we can obtain a characterization of the optimal control.

**Theorem 5.3.** *Let* $v^*$*be an optimal control of* (2.4)-(2.8) *and let* $w^* \in W^{1,2}$ *with* $w_i^* \in L$ *for* $i = 1, 2, 3, 4$ *be the optimal state, that is* $w^*$ *is the solution to*

(2.4)-(2.8) *with the control* $v^*$. *Then,*

$$v^* = \min\left\{v^{\max}, \max\left(0, \frac{aw_1^* p_1 + aw_2^* p_2 - (aw_1^* + aw_2^*)\, p_4}{\eta}\right)\right\}. \tag{5.13}$$

*Proof.* We suppose $v^*$ is an optimal control and $w^* = (w_1^*, w_2^*, w_3^*, w_4^*) = (w_1, w_2, w_3, w_4)(v^*)$ are the corresponding state variables. Consider $v^\varepsilon = v^* + \varepsilon h \in U_{ad}$ and corresponding state solution $w^\varepsilon = (w_1^\varepsilon, w_2^\varepsilon, w_3^\varepsilon, w_4^\varepsilon) = (w_1, w_2, w_3, w_4)(v^\varepsilon)$, we have

$$\begin{aligned}
&J'(v^*)(h)\\
&= \lim_{\varepsilon\to 0}\frac{1}{\varepsilon}\left(J(v^\varepsilon) - J(v^*)\right)\\
&= \lim_{\varepsilon\to 0}\frac{1}{\varepsilon}\Big(\int_0^T\int_\Omega \rho_1\left(w_2^\varepsilon - w_2^*\right)(t,r)\,drdt\\
&\quad + \int_0^T\int_\Omega \rho_2\left(w_3^\varepsilon - w_3^*\right)(t,r)\,drdt\Big) + \frac{\eta}{2}\int_0^T\int_\Omega \left((v^\varepsilon)^2 - (v^*)^2\right)(t,r)\,drdt\\
&= \lim_{\varepsilon\to 0}\Big(\int_0^T\int_\Omega \rho_1\left(\frac{w_2^\varepsilon - w_2^*}{\varepsilon}\right)(t,r)\,drdt + \int_0^T\int_\Omega \rho_2\left(\frac{w_3^\varepsilon - w_3^*}{\varepsilon}\right)(t,r)\,drdt\\
&\quad + \frac{\eta}{2}\int_0^T\int_\Omega \left(\varepsilon(h)^2 + 2hv^*\right)(t,r)\,drdt\Big)\\
&= \int_0^T\int_\Omega \rho_1 W_2(t,r)\,drdt + \int_0^T\int_\Omega \rho_2 W_3(t,r)\,drdt + \eta\int_0^T\int_\Omega (h^*v^*)(t,r)\,drdt\\
&= \int_0^T \langle D\rho, DY\rangle_{H(\Omega)}\,dt + \int_0^T \langle \eta v^*, h\rangle_{L^2(\Omega)}\,dt.
\end{aligned} \tag{5.14}$$

We use (5.1) and (5.12), we have

$$\begin{aligned}
\int_0^T \langle D\rho, DY\rangle_{H(\Omega)}\,dt &= \int_0^T \langle D^*D\rho, W\rangle_{H(\Omega)}\,dt\\
&= \int_0^T \left\langle -\frac{\partial p}{\partial t} - Ap - H^*p, W\right\rangle_{H(\Omega)} dt\\
&= \int_0^T \left\langle p, \frac{\partial W}{\partial t} - AW - HW\right\rangle_{H(\Omega)} dt\\
&= \int_0^T \langle p, Gh\rangle_{H(\Omega)}\,dt\\
&= \int_0^T \langle G^*p, h\rangle_{L^2(\Omega)}\,dt.
\end{aligned} \tag{5.15}$$

Since $J$ is Gateaux differentiable at $v^*$ and $U_{ad}$ is convex, as the minimum of the objective functional is attained at $v^*$ it is seen that $J^{'}(v^*)(u-v^*) \geq 0$ for all $u \in U_{ad}$ .

We take $h = u - v^*$ and we use (5.14)-(5.15), then

$$J^{'}(v^*)(u-v^*) = \int_0^T \langle G^*p + \rho u^*, (u-v^*)\rangle_{L^2(\Omega)}\, dt.$$

We conclude that $J^{'}(v^*)(u-v^*) \geq 0$ equivalent to

$$\int_0^T \langle G^*p + \eta v^*, (u-v^*)\rangle_{L^2(\Omega)}\, dt \geq 0$$

for all $u \in U_{ad}$. By standard arguments varying $u$, we obtain

$$\eta v^* = -G^*p.$$

Then

$$v^* = \frac{ay_1^*p_1 + ay_2^*p_2 - (ay_1^* + ay_2^*)\,p_4}{\eta}.$$

As $v^* \in U_{ad}$, we have

$$v^* = \min\left\{v^{\max},\ \max\left(0, \frac{ay_1^*p_1 + ay_2^*p_2 - (ay_1^* + ay_2^*)\,p_4}{\eta}\right)\right\}.$$

□

## 6. Numerical results

6.1. **Algorithm and initial values of the model parameters.** This section presents numerical simulations that demonstrate the theoretical results discussed in the previous sections, focusing on our spatiotemporal vaccine strategy for a system involving partial differential equations (PDEs). To solve our optimal system, which consists of the state system (2.4)-(2.8), the dual system (5.12), and the control characterization (5.13), we employed a discrete iterative scheme that converges via an appropriate test, similar to the forward-backward-sweep method (FBSM) [24]. We utilized the explicit Euler discretization method to solve the forward-in-time state system with the initial hypothesis. In contrast, we solved the backward-in-time dual system due to the transversal condition. To demonstrate our approach, we utilized MATLAB software as a computational tool. To approximate the second-order spatial derivatives $\triangle S_d$, $\triangle E_d$, $\triangle I_d$ and $\triangle R_d$, we applied the second-order explicit Euler method. Subsequently, we updated the optimal control values based on the variable state and adjoint values obtained in the previous steps. Finally, we repeated these steps until we reached a defined tolerance criterion. As mentioned in paragraph 2.1, it has been established that the severity of the disease is contingent upon the original subdomain. In the following

paragraphs, we will distinguish between two cases: (1) where the infection originates from the lower-left corner, and (2) where it starts from the middle of the domain . We assume that the susceptible population is uniformly distributed, with 20 individuals in each cell of $1km \times 1km$, However, in the original cell of the diseases spread ($\Omega_1$, where the disease begins in the lower-left corner of $\Omega$ and $\Omega_2$, where the disease begins in the middle of $\Omega$), there are 4 exposed, 4 infected, 2 recovered, and 10 susceptible individuals. Our choice of a density of 6 individuals per $km^2$ is based on the findings of the study titled "Reemerging Rabies and Lack of Systemic Surveillance in the Peoples Republic of China" [38]. In that study, the authors estimated that densities varied by habitat, ranging from $(8-20\ dogs/km^2)$, In this study, we consider a high-contact situation with a population density of 20. We choose a rectangular grid of dimensions 40 km x 40 km as the domain . The values of the parameters and initial conditions are provided in Table 2 and 3, sourced from [39, 27]. We set the upper limit of the optimality condition as $v^{max} = 1$ [12], and adopt the constant weight values in the objective function as $\rho_1 = 1$, $\rho_2 = 1$, and $\eta = 2$, taken from [4].

| Notations | Value | Description($Units$) |
|---|---|---|
| $\Lambda$ | $2.34 \times 10^5$ | $Dog\ birth\ population\ \left(month^{-1}\right)$ |
| $\lambda$ | $\frac{1}{6}$ | $Dog\ loss\ rate\ of\ immunity\ \left(\left(people/km^2\right)^{-1}.month^{-1}\right)$ |
| $i$ | 1.045 | $Dog\ incubation\ period\ \left(month^{-1}\right)$ |
| $\sigma$ | $\frac{1}{1.045}$ | $\frac{1}{i}$ |
| $\gamma$ | 0.49 | $Clinical\ outcome\ rate\ of\ exposed\ dogs\ \left(month^{-1}\right)$ |
| $m$ | 0.0064 | $Dog\ natural\ mortality\ rate\ \left(month^{-1}\right)$ |
| $\beta_{dd}$ | $11.34 \times .10^6$ | $Dog\ to-dog\ transmission\ rate\ \left(month^{-1}\right)$ |

TABLE 2. Initial conditions and parameters values

| | | |
|---|---|---|
| $k$ | 0.09 | $Dog\ vaccination\ rate$ $\left(month^{-1}\right)$ |
| $\mu$ | 1 | $Dog\ disease-related$ $death\ rate$ $\left(month^{-1}\right)$ |
| $d_1$ | 0.005 | $Diffusion\ rate\ for$ $the\ susceptible\ dogs$ $\left(km^2/month\right)$ |
| $d_2$ | 0.01 | $Diffusion\ rate\ for$ $the\ exposed\ dogs$ $\left(km^2/month\right)$ |
| $d_3$ | 0.01 | $Diffusion\ rate\ for$ $the\ infected\ dogs$ $\left(km^2/month\right)$ |
| $d_4$ | 0.005 | $Diffusion\ rate\ for$ $the\ recovered\ dogs$ $\left(km^2/month\right)$ |
| $t$ | $[1, 150]$ | $time\ period$ $(month)$ |

TABLE 3. Initial conditions and parameters values

6.2. **Discussion.** Figures 1 to 4 illustrate the numerical outcomes for the susceptible, exposed, infected, and recovered groups, respectively. We conducted simulations for two scenarios: one where the disease initiated from the corner (1) and the other from the middle (2). In both cases, the disease spreads from susceptible individuals to exposed individuals, and after an incubation period, to infected individuals, eventually affecting the entire population. However, in the second scenario, the disease spreads faster, demonstrating the heightened risk when it originates from the middle. This emphasizes the significance of the spatial component utilized in our model. Additionally, only a small number of individuals (approximately 4) recovered from the disease. The insights gained from these simulations have led us to consider developing an effective control strategy based on these findings. In response, we propose the implementation of an optimal control vaccine, which specifically targets the transmission of the disease.

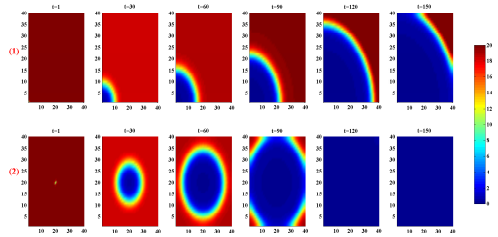

FIGURE 1. Susceptible behavior without control

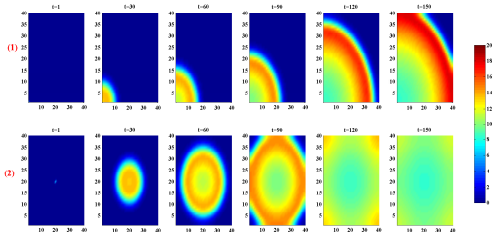

FIGURE 2. Exposed behavior without control

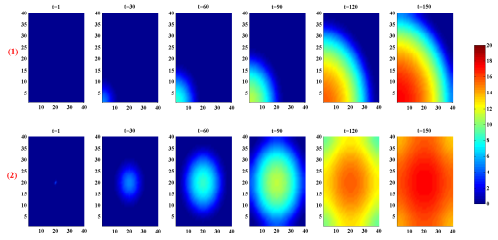

FIGURE 3. Infected behavior without control

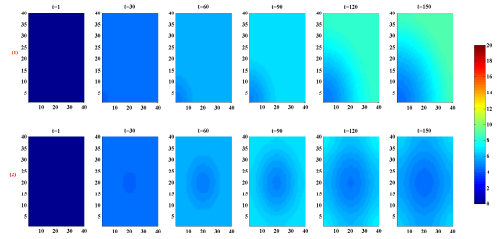

FIGURE 4. recovered behavior without control

To demonstrate the significance of the vaccination strategy, we examine two cases:

(1) In the first case, we take a more realistic approach and assume that the vaccine campaign commences from the 50th month.
(2) In the second case, we consider the vaccine distribution starting from the first month of the disease.

6.2.1. The vaccine strategy starts after the 50th months. In order to evaluate the effectiveness of the spatiotemporal vaccine strategy, we analyze the prevalence of infection over 150 months [41]. For a more realistic scenario, we simulate the spread of the infection for $t = 50$ months without any intervention and then calculate the optimal vaccination strategy starting from $t = 51$ months based on the infection progression then. Figures 5, 6, 7, and 8 clearly demonstrate the significant impact of our spatiotemporal vaccine strategy in slowing the spread of infection. In particular, Figure 6 shows that the density of infected dogs increases from 18 to 2 after 150 months with optimal control except at the source of infection. The remarkable impact of the optimal control strategy is further reflected in Figure 8, where the maximum number of restored dogs is approximately 18, compared to less than 4 in the absence of control, emphasizing the importance of our control strategy. Additionally, both Figures 1 and 5 show the disappearance of the susceptible dog population in both cases, with or without vaccination. In the absence of vaccination, susceptible dogs are transferred to infected individuals as shown in Figure 3. On the other hand, the vaccination strategy adopted in this work transfers susceptible dogs to the restored class through the mechanism shown in Figure 8.

In Figures 5, 6, 7, and 8, when we use our spatiotemporal vaccine. The impact of the optimal control strategy is very remarkable in slowing the spread of the infection. In fact, in Figure 6, after 150 months, the density of the infected population increases from 18 infected dogs in the absence of control to 2 infected in the presence of optimal control except at the source area of infection. In Figure 8, the maximum number of dogs restored to approximately 18 dogs against less than 4 dogs in the absence of control, which is very beneficial and reflects the importance of our control strategy.

It can be seen in Figures 1 and 5 that the rabies susceptible dog population disappeared in both cases, either in the absence or in the presence of a vaccine. In the first case, susceptible dogs are transferred to infected individuals (see Figure 3). But in the second case, susceptible dogs are transferred to the restored class (see Figure 8) through the mechanism of the vaccine strategy. adopted in this work.

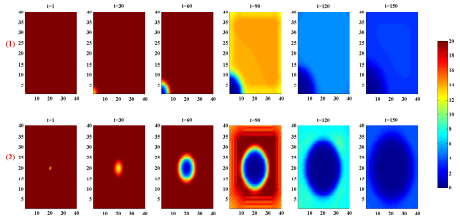

FIGURE 5. Susceptible behavior with control (vaccine strategy starts after the 50th month)

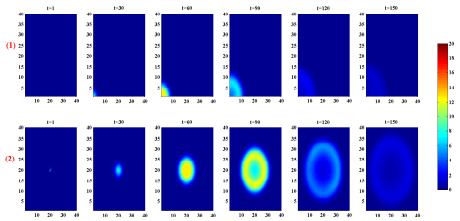

FIGURE 6. Exposed behavior with control (vaccine strategy starts after the 50th month)

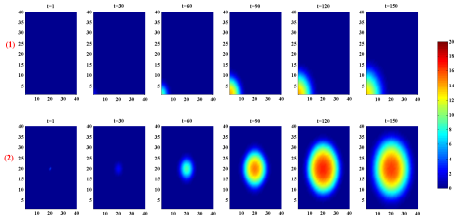

FIGURE 7. Removed behavior with control (vaccine strategy starts after the 50th month)

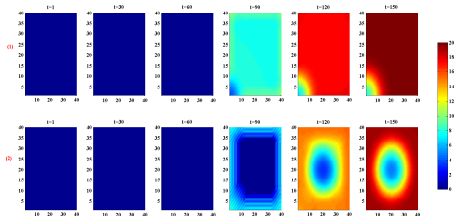

FIGURE 8. Removed behavior with control (vaccine strategy starts after the 50th month)

6.2.2. The vaccine strategy starts from the first month. In this subsection, we aim to demonstrate the impact of the intervention time on the vaccine strategy. To this end, we present the results of optimal vaccination in Figures 9 and 10, starting from the month t=1 when rabies is first detected in the study area. The effectiveness of the vaccine in controlling the spread of rabies is observed. Comparing these results with those obtained in the case of applying the vaccine after 50 months, we can conclude that the efficiency of the vaccine increases as we apply it earlier.

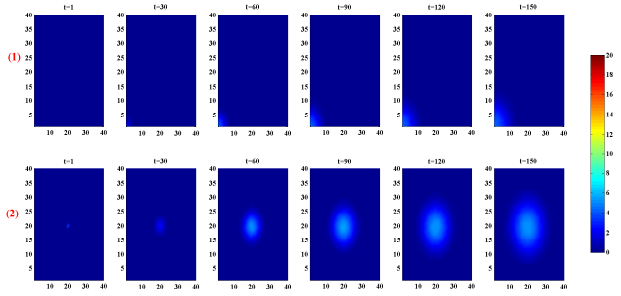


FIGURE 9. Infected behavior with control ( vaccine strategy starts from the first month)

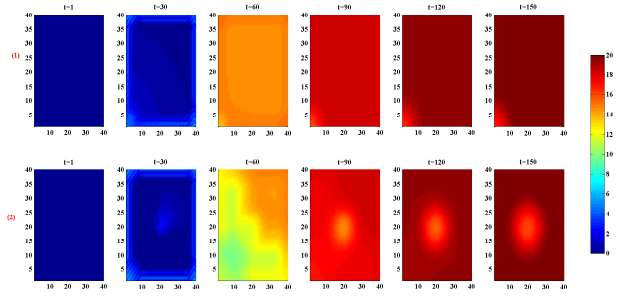


FIGURE 10. Removed behavior with control ( vaccine strategy starts from the first month)

## 7. Conclusion

In this study, we have presented a comprehensive spatiotemporal model of rabies disease in dogs, incorporating the dynamics of disease spread in a two-dimensional space. By considering the spatial factor in our model, we aimed

to capture the realistic propagation of the epidemic and its implications for disease control strategies.

Our simulations demonstrated that the disease exhibits a characteristic pattern, originating from a source area and gradually spreading to other regions in the absence of control measures. Importantly, we observed that the initial location of the outbreak significantly influences its subsequent progression. Initiating the outbreak from the central area led to more severe consequences compared to starting from a lateral area. This finding underscores the importance of spatial considerations in understanding and managing rabies outbreaks.

To address the challenge of disease control, we developed and evaluated a vaccination-based strategy. Our simulations indicated that timely administration of vaccines during the early stages of the outbreak was crucial for effective containment. By targeting susceptible individuals, the vaccination strategy successfully reduced the number of infected and exposed dogs, while promoting the recovery of affected individuals. These findings highlight the critical role of proactive vaccination campaigns in mitigating the spread of rabies in dog populations.

From a mathematical standpoint, we established the existence of positive and bounded solutions for the state system, providing a solid foundation for our modeling approach. Furthermore, we employed control theory to identify an optimal control strategy that minimizes the number of infected and exposed dogs, as well as the associated vaccination costs. Through the analysis of state functions and adjoint functions, we characterized the optimal control and demonstrated its efficacy in curbing the disease spread.

In conclusion, this study contributes valuable insights into the spatiotemporal dynamics of rabies disease in dogs. By incorporating spatial considerations and developing a vaccination-based control strategy, we offer practical recommendations for mitigating the spread of rabies. These findings have implications for public health policies and intervention strategies aimed at reducing the burden of rabies in dog populations. Further research and collaboration are warranted to refine and validate our model and to explore additional factors that may influence disease dynamics in different contexts.

**Data availability:** The source code and datasets generated and analyzed during the current study are available in [27, 39].

## References

[1] L.J. Allen, D.A. Flores, R.K. Ratnayake and J.R. Herbold, *Discrete-time deterministic and stochastic models for the spread of rabies*, Appl. Math. Comput., **132**(2-3) (2002), 271–292.

[2] R.M. Anderson and R.M. et May, *Infectious diseases of humans*, dynamics and control, OUP Oxford, Medical, (1991), 757 pages.
[3] M. Artois, M. Langlais and C. Suppo, *Simulation of rabies control within an increasing fox population,* Ecological Mod., **97**(1-2) (1997), 23–34.
[4] J.K.K. Asamoah, F.T. Oduro, E. Bonyah and B. Seidu, *Modelling of rabies transmission dynamics using optimal control analysis,* J. Appl. Math., (2017), https://doi.org/10.1155/2017/2451237.
[5] V. Barbu, *Mathematical methods in optimization of differential systems*, Springer Science & Business Media, **310** (1994).
[6] Y. Benfatah, A. El Bhih, M. Rachik and A. Tridane, *On the Maximal Output Admissible Set for a Class of Bilinear Discrete-time Systems,* Int. J. Control Autom. Syst., vol. 19, (2021), pp. 35513568, https://doi.org/10.1007/s12555-020-0486-6.
[7] H. Brezis, P.G. Ciarlet and J.L. Lions, *Analyse fonctionnelle: thorie et applications*, vol. 91, Dunod, Paris, (1999).
[8] J. Chen, L. Zou, Z. Jin, and S. Ruan, *Modeling the geographic spread of rabies in China*, PLoS Neglected Tropical Diseases, **9**(5) (2015).
[9] N.N. Chidumayo, *System dynamics modelling approach to explore the effect of dog demography on rabies vaccination coverage in Africa*, PLoS One, **13**(10) (2018).
[10] J.E. Childs, A.T. Curns, M.E. Dey, L.A. Real, L. Feinstein, O.N. Bjrnstad and J.W. Krebs, *Predicting the local dynamics of epizootic rabies among raccoons in the United States*, Appl. Math. Comput., **216**(2) (2010), 395–409.
[11] S. Chinviriyasit and W. Chinviriyasit, *Numerical modelling of an SIR epidemic model with diffusion*, Appl. Math. Comput., **216**(2) (2010), 395–409.
[12] T. Clayton, S.D. Sylvester, L.J. Gross, S. Lenhart and L.A. Real, *Optimal control of a rabies epidemic model with a birth pulse*, J. Biol. Dyn., **4**(1) (2010), 43–58.
[13] M. Coyne, G. Smith and F.E. McAllister, *Mathematic model for the population biology of rabies in raccoons in the mid-Atlantic states*, Am. J. Vet. Res., **50**(12) (1989), 2148–2154.
[14] B. Dharmalingam and L. Jothi, *RDIS: The Rabies Disease Information System*, Bioinformation, **11**(11) (2015), 506.
[15] D.T. Dimitrov, T.G. Hallam, C.E. Rupprecht, A.S. Turmelle and G.F. McCracken, *Integrative models of bat rabies immunology, epizootiology and disease demography*, J. Theor. Biol., **245**(3) (2007), 498–509.
[16] N.D. Evans and A.J. Pritchard, *A control theoretic approach to containing the spread of rabies*, Math. Med. Biol., **18**(1) (2001), 1–23.
[17] K. Hampson, J. Dushoff, J. Bingham, G. Brckner, Y.H. Ali and A. Dobson, *Synchronous cycles of domestic dog rabies in sub-Saharan Africa and the impact of control efforts*, Proc. Natl. Acad. Sci. U. S. A., **104**(18) (2007), 7717–7722.
[18] A. Källen, P. Arcuri and J.D. Murray, *A simple model for the spatial spread and control of rabies*, J. Theor. Biol., **116**(3) (1985), 377–393.
[19] K.I. Kim, Z. Lin and L. Zhang, *Avian-human influenza epidemic model with diffusion*, Nonlinear Anal. Real World Appl., **11**(1) (2010), 313–322.
[20] A.E.A. Laaroussi, A. El Bhih and M. Rachik, *Optimal vaccination and treatment policies with constrained inequalities to study limited vaccination resources for a multistrain reaction diffusion SEIR model of COVID-19*, Partial Differ. Equ. Appl. Math., **10** (2024), 100684, https://doi.org/10.1016/j.padiff.2024.100684.
[21] A.E.A. Laaroussi, R. Ghazzali, M. Rachik and S. Benrhila, *Modeling the spatiotemporal transmission of Ebola disease and optimal control: a regional approach*, Int. J. Dyn. Control, **7**(3) (2019), 1110–1124.

[22] A.E.A. Laaroussi, M. Rachik and M. Elhia, *An optimal control problem for a spatiotemporal SIR model*, Int. J. Dyn. Control, **6** (2018), 384–397.
[23] E.M. Lotfi, M. Maziane, K. Hattaf and N. Yousfi, *Partial differential equations of an epidemic model with spatial diffusion*, Int. J. Partial Differ. Equ., (2014).
[24] M. Michael, M. Libin and H. Weimin, *Convergence of the forward-backward sweep method in optimal control*, Comput. Optim. Appl., **53**(1) (2012), 207–226.
[25] R.M. Neilan and S. Lenhart, *Optimal vaccine distribution in a spatiotemporal epidemic model with an application to rabies and raccoons*, J. Math. Anal. Appl., **378**(2) (2011), 603–619.
[26] A. Pazy, *Semigroups of linear operators and applications to partial differential equations*, vol. 44, Springer Science and Business Media, (2012).
[27] S. Ruan, *Spatiotemporal epidemic models for rabies among animals*, Infect. Dis. Model., **2**(3) (2017), 277–287.
[28] C.E. Rupprecht, C.A. Hanlon and T. Hemachudha, *Rabies re-examined*, Lancet Infect. Dis., **2**(6) (2002), 327–343.
[29] C.A. Russell, L.A. Real and D.L. Smith, *Spatial control of rabies on heterogeneous landscapes*, PLoS One, **1**(1) (2006).
[30] K.F. Smith, A.P. Dobson, F.E. McKenzie, L.A. Real, D.L. Smith and M.L. Wilson, *Ecological theory to enhance infectious disease control and public health policy*, Front. Ecol. Environ., **3**(1) (2005), 29–37.
[31] G.C. Smith and S. Harris, *Rabies in urban foxes (Vulpes vulpes) in Britain: the use of a spatial stochastic simulation model to examine the pattern of spread and evaluate the efficacy of different control regimes*, Philos. Trans. R. Soc. Lond. B Biol. Sci., **334**(1271) (1991), 459–479.
[32] D.L. Smith, B. Lucey, L.A. Waller, J.E. Childs and L.A. Real, *Predicting the spatial dynamics of rabies epidemics on heterogeneous landscapes*, Proc. Natl. Acad. Sci. USA, **99**(6) (2002), 3668–3672.
[33] J. Smoller, *Shock waves and reactiondiffusion equations*, vol. 258, Springer Science and Business Media, (2012).
[34] J.H. Swart, *Hopf bifurcation and stable limit cycle behavior in the spread of infectious disease, with special application to fox rabies*, Math. Biosci., **95**(2) (1989), 199–207.
[35] H.H. Thulke, V. Grimm, M.S. Mller, C. Staubach, L. Tischendorf, C. Wissel and F. Jeltsch, *From pattern to practice: a scaling-down strategy for spatially explicit modelling illustrated by the spread and control of rabies*, Ecol. Model., **117**(2-3) (1999), 179–202.
[36] I.I. Vrabie, *$C_0$-semigroups and applications*, vol. 191 of North-Holland Mathematics Studies, (2003).
[37] X.K. Wei, Y. Xiong, X.N. Li, M. Zheng, Y. Pan, X.X. He, J.J. Liang, C. Liu, Y.Z. Zhong, L.B. Zou, et al., *Vaccination demonstration zone successfully controls rabies in Guangxi province, China*, BMC Infect. Dis., **18**(1) (2018), 386.
[38] X. Wu, R. Hu, Y. Zhang, G. Dong and C.E. Rupprecht, *Reemerging rabies and lack of systemic surveillance in Peoples Republic of China*, Emerg. Infect. Dis., **15**(8) (2009), 1159.
[39] J. Zhang, Z. Jin, G.Q. Sun, X. Sun and S. Ruan, *Spatial spread of rabies in China*, J. Appl. Anal. Comput, **2** (2012), 111–126.
[40] J. Zhang, Z. Jin, G.Q. Sun, T. Zhou and S. Ruan, *Analysis of rabies in China: transmission dynamics and control*, PLoS One, **6**(7) (2011).
[41] J. Zinsstag, S. Drr, M.A. Penny, R. Mindekem, F. Roth, S M. Gonzalez, S. Naissengar and J. Hattendorf, *Transmission dynamics and economics of rabies control in dogs and humans in an African city*, Proc. Natl. Acad. Sci. USA, **106**(35) (2009), 14996–15001.